Modelling the vegetation of China using the process-based equilibrium terrestrial biosphere model BIOME3

Jian Ni, Martin Sykes, I. Colin Prentice, Wolfgang Cramer

Modelling the vegetation of China using the process-based equilibrium terrestrial biosphere model BIOME3

JIAN NI*†, MARTIN T. SYKES*, I. COLIN PRENTICE*‡ and WOLFGANG CRAMER§ *Climate Impacts Group, Department of Ecology, Lund University, Ecology Building, Sölvegatan 37, S-223 62 Lund, Sweden. E-mail: martin@planteco.lu.se, †Laboratory of Quantitative Vegetation Ecology, Institute of Botany, Chinese Academy of Sciences, Xiangshan Nanxincun 20, 100093 Beijing, P.R. China. E-mail: nijian@public.east.cn.net, ‡Max Planck Institute for Biogeochemistry, Postfach 10 01 64, D-07701 Jena, Germany. E-mail: cprentic@bgc-jena.mpg.de, §Potsdam Institute for Climate Impact Research, Telegrafenberg, PO Box 60 12 03, D-14412 Potsdam, Germany. E-mail: wolfgang.cramer@pik-potsdam.de

ABSTRACT

1 We model the potential vegetation and annual net primary production (NPP) of China on a 10′ grid under the present climate using the processed-based equilibrium terrestrial biosphere model BIOME3. The simulated distribution of the vegetation was in general in good agreement with the potential natural vegetation based on a numerical comparison between the two maps using the ΔV statistic (ΔV = 0.23). Predicted and measured NPP were also similar, especially in terms of biome-averages.

2 A coupled ocean–atmosphere general circulation model including sulphate aerosols was used to drive a double greenhouse gas scenario for 2070–2099. Simulated vegetation maps from two different CO_2 scenarios (340 and 500 p.p.m.v.) were compared to the baseline biome map using ΔV. Climate change alone produced a large reduction in desert, alpine tundra and ice/polar desert, and a general pole-ward shift of the boreal, temperate deciduous, warm–temperate evergreen and tropical forest belts, a decline in boreal deciduous forest and the appearance of tropical deciduous forest. The inclusion of CO_2 physiological effects led to a marked decrease in moist savannas and desert, a general decrease for grasslands and steppe, and disappearance of xeric woodland/scrub. Temperate deciduous broadleaved forest, however, shifted north to occupy nearly half the area of previously temperate mixed forest.

3 The impact of climate change and increasing CO_2 is not only on biogeography, but also on potential NPP. The NPP values for most of the biomes in the scenarios with CO_2 set at 340 p.p.m.v. and 500 p.p.m.v. are greater than those under the current climate, except for the temperate deciduous forest, temperate evergreen broadleaved forest, tropical rain forest, tropical seasonal forest, and xeric woodland/scrub biomes. Total vegetation and total carbon is simulated to increase significantly in the future climate scenario, both with and without the CO_2 direct physiological effect.

4 Our results show that the global process-based equilibrium terrestrial biosphere model BIOME3 can be used successfully at a regional scale.

Key words BIOME3 model, biome pattern, carbon storage, Chinese vegetation, climate change and CO_2 enrichment, ΔV statistic, net primary production, prediction evaluation.

Correspondence: Dr Jian Ni, Global Ecology Group, Max Planck Institute for Biogeochemistry, Postfach 10 01 64, D-07701 Jena, Germany. E-mail: jni@bgc-jena.mpg.de

INTRODUCTION

Climate change driven by higher atmospheric concentrations of greenhouse gases is expected to affect the terrestrial biosphere through linked changes in vegetation distribution and net primary production (NPP), with concomitant changes in terrestrial carbon storage (Melillo *et al.*, 1996). Previous modelling studies have examined separately the effects of climate on vegetation distribution, using biogeography models (e.g. Prentice *et al.*, 1992; Smith *et al.*, 1992; Claussen & Esch, 1994; Prentice & Sykes, 1995), and the effects of climate and CO_2 on NPP using biogeography models (e.g. Melillo *et al.*, 1993; Melillo, 1995). A continental-scale study, the VEMAP project (VEMAP Members, 1995), demonstrated the interdependence of the biogeographical and biogeochemical aspects of the ecological response, showing that any serious attempt to assess how global change will affect natural ecosystems must include both aspects (VEMAP Members, 1995).

The process-based equilibrium terrestrial biosphere model BIOME3 (Haxeltine & Prentice, 1996) combines biogeographical and biogeochemical modelling approaches within a single global framework to simulate vegetation distribution and biogeochemistry. Comparison with the mapped distributions of global vegetation showed that the model successfully reproduced the broad-scale patterns in potential natural vegetation distribution. At the regional scale, however, some of the modelled vegetation patterns did not agree particularly well with the potential natural vegetation distribution. In China, for example, the boundary between temperate deciduous broadleaved forest and warm–temperate evergreen broadleaved/mixed forest, the area of desert, and the vegetation of the Tibetan Plateau, were poorly simulated. A number of reasons can be used to explain this lack of correlation at the regional scale, including lower resolution climate data, sparse data coverage, strong spatial variation, and errors in the global climate, soil texture and vegetation databases for China.

Most of the main vegetation types of the world can be found within China (Editorial Committee for Vegetation of China, 1980). China covers about 10% of the total world area. Thus, the response of Chinese vegetation to rapid environmental change is important, both regionally and globally. Climate–vegetation interactions have been studied in China, using Holdridge's life-zone scheme for global change (Zhang & Yang, 1993) and by simulating NPP (Zhang & Yang, 1990), in each case, however, using only a statistical modelling approach. Hulme *et al.* (1992) predicted the distributions of nine vegetation types under current climate and their response to changed climate in 2050 by using a coupled general circulation model (GCM). This was again a statistical approach and, moreover, the number of vegetation categories was small and the geographical resolution was very coarse.

More detailed and accurate regional climate, soils and vegetation data of China are newly available and we apply the BIOME3 model using these regional data to predict the potential vegetation distribution and annual NPP of China under the present climate. The simulated vegetation distribution is then compared with the potential natural vegetation using the ΔV statistic (Sykes *et al.*, 1999). We also simulate the equilibrium vegetation under a future climate scenario using output from the Hadley Climate Centre coupled ocean–atmosphere General Circulation Model including aerosols (Mitchell *et al.*, 1995; Johns *et al.*, 1997) with CO_2 modelled at 340 and 500 p.p.m.v.

METHODS

The BIOME3 model

The equilibrium terrestrial biosphere model, BIOME3 (Haxeltine & Prentice, 1996), simulates the direct effects of CO_2 on photosynthesis, stomatal conductance and leaf area through the application of an interactively coupled carbon and water flux model (Haxeltine *et al.*, 1996). The model relies on ecophysiological constraints, resource availability and competition among plant functional types (PFTs) to simulate potential vegetation distribution and NPP, and to predict responses of vegetation to climate change alone and both climate change and CO_2 enrichment (Haxeltine & Prentice, 1996; Haxeltine, 1996). Model inputs are atmospheric CO_2 concentration, latitude, soil texture, absolute minimum temperature, and monthly climate data (temperature, precipitation and sunshine). Model outputs include a

quantitative vegetation state description in terms of the dominant and secondary PFTs present, which can then be classified into biome types, along with the total LAI and NPP for the ecosystem.

The model has been tested for the present climate by comparison with a global map of natural vegetation, NPP measurements, and global data on the fraction of photosynthetically active radiation (FPAR) absorbed by vegetation (Haxeltine & Prentice, 1996).

Climate and soil texture data

Monthly mean and absolute minimum temperature, precipitation, and percent of sunshine hours data for 841 standard weather stations between 1951 and 1980 in China (Chinese Central Meteorological Office, 1984) were interpolated to a 10′ latitude × 10′ longitude grid by the smoothing spline method of Hutchinson (1989). Climate station data from western China were, however, sparse, especially for the Tibetan Plateau, where there is a strong spatial variation, but the number of climate stations here are more than those in the world climate database.

A soil-texture dataset of China was constructed on the 10′ grid, based on textural information digitized from Xiong & Li (1987). The data set distinguishes 12 classes of fine-, medium- and coarse-textured soils and combinations of these classes were assigned to the seven categories used in BIOME3 (Table 1).

Table 1 Assignments from the 12 soil texture classes of China (Xiong & Li, 1987) to the seven categories used by BIOME3 (Haxeltine & Prentice, 1996)

Soil texture classes of BIOME3	Soil texture classes of China
Coarse	Rocks, sands, coarse-sands
Medium–coarse	Fine sands
Fine-coarse	Loamy sands
Fine–medium–coarse	Sandy loams
Medium	Loams, silty loams
Fine–medium	Clay loams, silty clay loams
Fine	Clay loams, clay

Vegetation data

A map of potential natural vegetation of China (Fig. 1a) on 10′ grid cell was devised for comparison with the simulated output from BIOME3. A digital vegetation map, which consists of 113 vegetation type units digitized from the 'Vegetation Map of the People's Republic of China' at 1 : 4000 000 scale (Hou *et al.*, 1982), was constructed by assigning these units to the 18 BIOME3 categories (Table 2).

The vegetation data of 113 units and 18 categories, climate and soil data are available via anonymous ftp to Department of Ecology, Plant Ecology, Lund University of Sweden <ftp:/dunbeatle.planteco.lu.se/pub/jian/chinadata>.

There were some problems in this assignment. First, the number of vegetation types were many more than the number of biomes. It was also difficult in some cases to determine which vegetation types should be assigned to a particular biome, because definitions are not the same between China and the rest of the world, e.g. for steppe, grassland and desert. Moreover, some of the mapped 113 vegetation types are mixtures, for example, larch forests that were assigned to boreal deciduous forest (Table 2) in the 'actual' vegetation map are mixtures of larch and boreal evergreen while birch forests are actually mixtures of broad-leaved summer-green and coniferous evergreen (Hou *et al.*, 1982).

Secondly, the digital vegetation map is of actual vegetation, and BIOME3 maps potential vegetation. It was necessary therefore to assign cultivated vegetation types from the digitized map to potential biomes. We used bioclimatic criteria to do these assignments.

Thirdly, the boundary between some biomes in China and in the rest of the world is different, such as between tropical seasonal forest and tropical rain forest. This made it difficult to make some assignments. Therefore, where confusion existed we used the boundaries described in BIOME3.

Climate scenario

We used climate output from the Hadley Centre coupled ocean–atmosphere general circulation model (Mitchell *et al.*, 1995; Johns *et al.*, 1997), including the effects of both greenhouse gases

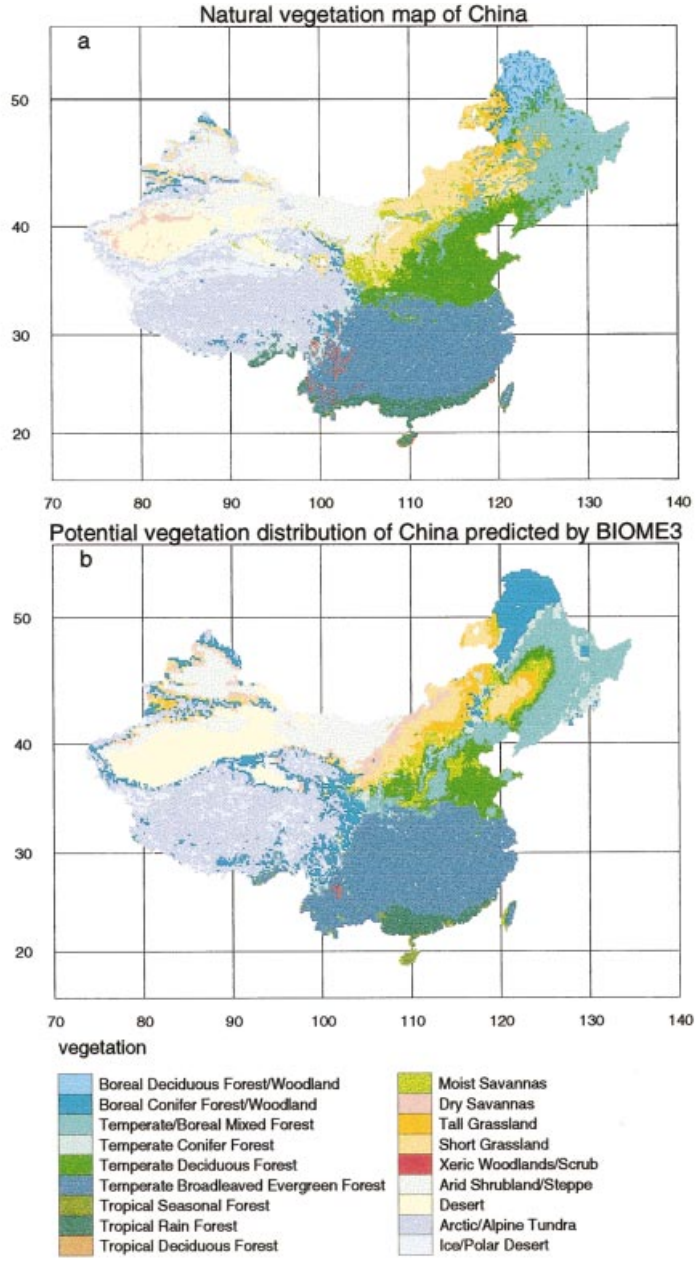

Fig. 1 Vegetation map of China. (a) Natural vegetation map of China, which consists of 18 BIOME3 categories assigned from 113 vegetation type units digitized from the 'Vegetation Map of the People's Republic of China' at 1 : 4000 000 scale (Hou *et al.*, 1982); and (b) potential vegetation map of China as predicted by BIOME3 (Haxeltine & Prentice, 1996).

Table 2 Allocation of the vegetation types and dominants of China (Editorial Committee for Vegetation of China, 1980; Hou *et al.*, 1982) to biomes for BIOME3 modelling and mapping

Biomes	Vegetation types
Boreal deciduous forest/woodland	Cold–temperate deciduous coniferous (*Larix*), broadleaved (*Betula*, *Populus*) forest
Boreal evergreen forest/woodland	*Picea–Abies* forest, *Pinus sylvestris* var. *mongolica*, meadow and cultivated vegetation in the boreal region
Temperate/boreal mixed forest	Temperate mixed deciduous broadleaved–evergreen coniferous forest (*Pinus koraiensis*, *Acer*, *Tilia*, *Fraxinus*, *Ulmus*, *Betula*) Cold–temperate deciduous broadleaved shrubland (*Corylus*, *Ostryopsis*, *Spiraea*) Cold–temperate cultivated vegetation, Graminoid meadow and swamp
Temperate conifer forest	Temperate evergreen coniferous forest (*Picea*, *Abies*, *Tsuga*) with *Rhododendron* montane scrub
Temperate deciduous forest	Temperate evergreen coniferous forest (*Pinus*) Temperate deciduous broadleaved/mixed forest (*Quercus*, *Cotinus*, *Pistacia*) Temperate deciduous broadleaved woodland/shrubland (*Vitex*, *Cotinus*, *Dalbergia*, *Exochorda*, *Quercus*) Temperate cultivated vegetation
Temperate broad-leaved evergreen forest	Warm–temperate evergreen coniferous forest (*Pinus*, *Cunninghamia*, *Cupressus*) Subtropical mixed deciduous–evergreen broadleaved forest (*Cyclobalanopsis*, *Platycarya*, *Castanopsis*, *Fagus*, evergreen oaks) Subtropical evergreen broadleaved forest (*Castanopsis*, *Cyclobalanopsis*, *Lithocarpus*, *Schima*, evergreen *Quercus*, *Phyllostachys*) Subtropical mixed deciduous–evergreen shrubland/scrub (*Rhododendron*, *Vaccinium*, *Platycarya*, *Zanthoxylum*) Subtropical cultivated vegetation
Tropical seasonal forest	Tropical seasonal forest (*Gironniera*, *Burretiodendra*, *Kleinhovia*, *Antiaris*)
Tropical rain forest	Tropical rain forest (*Vatica*, *Dipterocarpus*, *Pometia*, *Myristica*) Subtropical–tropical mixed deciduous–evergreen shrubland (*Melastoma*, *Aporosa*) Subtropical evergreen broadleaved forest with tropical trees (*Castanopsis*, *Schima*, Lauraceae) Tropical scrub or coppicewood (*Ficus*, *Alchornea*, *Boehmeria*) Tropical mangrove Tropical cultivated vegetation
Tropical deciduous forest	*Scaevola*, *Pisonia* in the islands of the South China Sea (the tropical deciduous forest occurs in the islands of South China Sea with a very small area. It does not exist in the mainland of China)
Moist savannas	*Ulmus* woodland on semiarid area Temperate forestry steppe/meadow (*Bothriochloa*, *Themeda*) Partly temperate cultivated vegetation
Dry savannas	*Populus* microphyllous woodland in arid areas Partly temperate cultivated vegetation
Tall grassland	Temperate forb–gramineous meadow steppe (*Filifolium*) Temperate steppe (*Stipa*, *Leymus*)
Short grassland	Temperate desert steppe (*Artimisia*, *Ajania*, *Caragana*) Temperate steppe (*Stipa*, *Festuca*)

Table 2 *continued.*

Biomes	Vegetation types
Xeric woodland/scrub	Subtropical or tropical savannas with thorny scrub
Arid shrubland/steppe	*Tamarix* scrub Temperate shrub desert (*Sympegma*, *Anabasis*, *Reaumuria*, *Artemisia*, *Kalidium*, *Ephedra*, *Zygophyllum*, *Nitraria*, *Caragana*, *Calligonum*, *Haloxylon*)
Desert	Temperate sandy desert Bare gobi, rocky hill, mobile sand-dune, salt crust
Arctic/alpine tundra	Montane scrub (*Salix*, *Vaccinium*, *Dasiphora*) Alpine scrub or cushion-like vegetation (*Arenaria*, *Androsace*) Alpine desert (*Caragana*, *Ceratoides*, *Ajania*) Alpine steppe (*Festuca*, *Stipa*, *Poa*) Alpine or subalpine meadow/swamp (*Kobresia*)
Ice/polar desert	Sparse vegetation with rocky fragments in Tibet Glaciers

and sulphate aerosols. The scenario was derived by computing the averages for 1931–1960 and for 2070–2099 from the climate model simulation and then interpolating the anomalies to our high-resolution grid. These were then added to the baseline climate to produce the climate fields used to drive BIOME3.

The doubled greenhouse gases simulation estimates an equilibrium climate corresponding to a doubling in the combined radiative forcing of all greenhouse gases. The emissions scenario (IPCC, 1996) included an increase in atmospheric CO_2 concentration from 340 to 500 p.p.m.v. and both these CO_2 concentrations were used for calculation of physiological CO_2 effects.

NPP data

Data on latitude, longitude, elevation, field measurements of stand age, leaf area index (LAI), total biomass and NPP for 690 sites were collected from forestry inventory data from 29 provinces supplied from the Forestry Ministry of China and found within the published literature (Ni *et al.*, unpublished data). Estimated NPP from field biomass measurement of Chinese forests were used in a comparison with modelled NPP. The forest types that were assigned to the biomes of BIOME3 were boreal deciduous forest, boreal evergreen forest, cold–temperate coniferous forest, temperate mixed coniferous and broadleaved deciduous forest, temperate deciduous broadleaved forest, temperate montane deciduous broadleaved forest, temperate tugai forest, warm–temperate evergreen broadleaved forest, warm–temperate mixed evergreen–deciduous broadleaved forest, warm–temperate sclerophyllous evergreen broadleaved forest, tropical rain forest and seasonal forest, temperate coniferous forest, and five major types of warm–temperate coniferous forests.

The NPP data set of Chinese forests, which is a contribution to the Global Net Primary Production Database Initiative (GPPDI), is available at the following web page: http://daacl.esd.ornl.gov/npq/chn/chf

ΔV statistic

The degree of change between two biome maps is usually measured by the fraction of cells that change biome class (Claussen & Esch, 1994), or by the kappa statistic (Monserud & Leemans, 1992) which has been widely used for comparison of vegetation maps (Prentice *et al.*, 1992; VEMAP Members, 1995; Haxeltine & Prentice, 1996).

Interpretation of the kappa statistic is less obvious when the aim is to quantify the amount of change between two maps derived using the same model. An attribute-based measure of

Table 3 Importance values for each plant life form used in the Δ V statistical calculation as assigned to the biomes

Biomes	Life form			
	Tree	Grass	Shrub	Bare ground
Boreal deciduous forest/woodland	1			
Boreal evergreen forest/woodland	1			
Temperate/boreal mixed forest	1			
Temperate conifer forest	1			
Temperate deciduous forest	1			
Temperate broadleaved evergreen forest	1			
Tropical seasonal forest	1			
Tropical rain forest	1			
Tropical deciduous forest	1			
Moist savannas	0.5	0.5		
Dry savannas		0.5	0.5	
Tall grassland		1		
Short grassland		1		
Xeric woodland/scrub	0.5		0.5	
Arid shrubland/steppe		0.25	0.25	0.5
Desert		0.125	0.125	0.75
Arctic/alpine tundra		0.5	0.5	
Ice/polar desert		0.125	0.125	0.75

dissimilarity between vegetation classes (ΔV) was therefore introduced by Sykes *et al*. (1999) as a non-trivial measure of dissimilarity between biomes. ΔV is based on (a) the relative importance of different plant life forms (e.g. tree, grass) in each class, and (b) a series of attributes (e.g. evergreen–deciduous, tropical–non-tropical) of each life form with a weight for each attribute. Dissimilarity beween two maps (ΔV) is obtained by area-weighted averaging of ΔV over the model grid. The resulting dissimilarity index is in the range from 0 to 1.

Implementation of ΔV requires the definition of plant life forms, assignment of importance values for life forms, definition of attributes, assignment of attribute values, and assignment of attribute weights. The definitions of plant life forms and attributes follow naturally from the structure of the model. Trees, grasses, shrubs, and bare ground were defined as the four plant life forms. The importance values and attribute values are estimates of the typical floristic composition of the biomes. Weighting the attributes is subjective because there is no biological basis for assigning relative significance. An implementation for BIOME3 is summarized in Tables 3 and 4.

RESULTS

Prediction of biome distributions and comparison to potential natural vegetation map

The model simulated a total of 17 unique biomes under current climate (Fig. 1b). Visual comparison of predicted biome distributions with their natural equivalents (Fig. 1a) shows a good agreement with a ΔV value (area-weighted averages across grid cells) of 0.23 (cf. Sykes *et al.*, 1999). Table 5 lists the ΔV values from this comparison for each biome.

BIOME3 predicted well some of the natural potential biomes such as temperate/boreal mixed forest, temperate deciduous forest, temperate broadleaved evergreen forest, tropical seasonal forest, tropical rain forest, arid shrubland/steppe and arctic/alpine tundra.

The boreal mixed biome still exists in areas of the Changbai and Xiaoxingan mountains in north-eastern China where boreal conifers and temperate summer-green trees are dominants. Additionally, an area of temperate deciduous forest is predicted correctly in central China, in northern Jiangsu Province and on the Shandong Peninsula.

Table 4 Attribute values and weights for plant life forms used by the ΔV statistic. Attributes with –99.9 for moist savannas and xeric woodland/shrub are derived later depending on dominant woody plant functional type

Life form	Attribute			
	Evergreen	Needle-leaf	Tropical	Boreal
Tree				
Boreal deciduous forest/woodland	0.00	0.75	0.00	1.00
Boreal evergreen forest/woodland	0.75	0.75	0.00	1.00
Temperate/boreal mixed forest	0.50	0.50	0.00	0.50
Temperate conifer forest	0.75	0.75	0.00	0.25
Temperate deciduous forest	0.00	0.25	0.00	0.00
Temperate broadleaved evergreen forest	0.75	0.25	0.00	0.00
Tropical seasonal forest	0.75	0.00	1.00	0.00
Tropical rain forest	1.00	0.00	1.00	0.00
Tropical deciduous forest	0.00	0.00	1.00	0.00
Moist savannas	–99.9	–99.9	–99.9	0.00
Xeric woodland/scrub	–99.9	–99.9	–99.9	0.00
(weights	0.2	0.2	0.3	0.3)
Grass	Warm	Arctic/alpine		
Tropical	1.00	1.00		
Desert	0.00	0.00		
Arctic/alpine tundra	0.00	1.00		
Ice/polar desert	0.00	1.00		
(weights	0.5	0.5)		
Shrub	Arctic/alpine			
Arctic/alpine tundra	1.00			
Ice/polar desert	1.00			
(weight	0.5)			
Bare ground (permafrost)	Arctic/alpine			
Ice/polar desert	1.00			
Others	0.00			
(weight	1)			

Temperate deciduous forest is predicted in areas of central eastern and north-eastern China where actually there is temperate cultivated vegetation. Warm–temperate broadleaved evergreen forest where warm–temperate evergreen trees, whether broad- or needleleaved, are dominant, is correctly predicted to occur over large areas, including southern and south-western China, Taiwan and at moderate elevations on the southern slope of the Himalayas. It is, however, predicted further north than it is currently found in this northern region, where the actual vegetation type is mixed evergreen–deciduous broadleaved forest.

Tropical seasonal forest is predicted to occur in several disjunct areas: southernmost Taiwan, Hainan Island, south-eastern coastal areas, and scattered areas on the south side of the Himalayas. Tropical rain forest is predicted to occur only in the south-easternmost part of the Chinese mainland and central and northern Taiwan, but this is north of its actual distribution as monsoon evergreen broadleaved forest: an ecotone between tropical rain forest and warm–temperate evergreen broadleaved forest (Editorial Committee for Vegetation of China, 1980). Tropical deciduous forest does not occur in the tropical mainland of China and the model does not predict any under the current climate.

There are some discrepancies regarding the boundaries among warm–temperate evergreen broadleaved forest, tropical rain forest and tropical seasonal forest (Haxeltine & Prentice, 1996).

Table 5 ΔV values of each biome used in comparisons between BIOME3 baseline simulations and natural potential vegetation, and between changed climate and baseline simulations. A) ΔV values from comparisons between actual vegetation distribution (Hou *et al.*, 1982) and potential biomes as predicted by BIOME3 under the current climate with CO_2 concentration at 340 p.p.m.v; B) ΔV values between potential vegetation division (Editorial Committee for Vegetation of China, 1980) and potential biome predicted by BIOME3 under current climate; C) ΔV values between biomes predicted by BIOME3 under current climate and those based on the scenario (2070–2099) with CO_2 concentration 340 p.p.m.v.; D) ΔV values for comparison between future biome distribution under a scenario with enhanced CO_2 concentration of 500 p.p.m.v. and simulated potential biomes under current climate with CO_2 concentration of 340 p.p.m.v.

Biomes	ΔV			
	A	B	C	D
Boreal deciduous forest/woodland	0.18	1.00	0.15	0.15
Boreal evergreen forest/woodland	0.36	0.51	0.30	0.28
Temperate/boreal mixed forest	0.18	0.28	0.05	0.23
Temperate conifer forest	0.40	0.43	0.29	0.23
Temperate deciduous forest	0.20	0.20	0.17	0.07
Temperate broadleaved evergreen forest	0.04	0.05	0.05	0.04
Tropical seasonal forest	0.20	0.11	0.03	0.03
Tropical rain forest	0.18	0.30	0.002	0
Tropical deciduous forest	—	—	1.00	1.00
Moist savannas	0.47	0.42	0.22	0.48
Dry savannas	0.63	0.42	0.11	0.45
Tall grassland	0.54	0.14	0.05	0.69
Short grassland	0.31	0.23	0.02	0.13
Xeric woodland/scrub	0.76	0.34	0.54	0.64
Arid shrubland/steppe	0.23	0.18	0.07	0.22
Desert	0.10	0.03	0.21	0.25
Arctic/alpine tundra	0.26	0.34	0.39	0.39
Ice/polar desert	0.66	0.63	0.67	0.67
Mean ΔV (weight = 1)	0.24	0.25	0.18	0.24
Mean ΔV (weight = consine latitude)	0.23	0.24	0.18	0.24

For example, seasonal forest is predicted for most of Hainan Island, which is mapped as true rain forest; rain forest is predicted for the northern part of southern China, although it should be warm–temperate evergreen broadleaved forest; and warm–temperate evergreen broadleaved forest is predicted for south-western China, where there are tropical seasonal and rain forests (Fig. 1a,b).

Arid shrubland/steppe includes all steppe, called desert steppe and steppe desert in the 'Vegetation of China' (Editorial Committee for Vegetation of China, 1980). These types were found under arid conditions in the temperate areas of north-western China. The model simulates these areas well. Deserts are correctly sited by the model in western China between the Tian mountains and the Tibetan Plateau. The alpine tundra is correctly predicted to occur in the Altai and Tian mountains and in Tibet.

There are some modelled biome distributions, such as boreal deciduous forest/woodland, boreal evergreen forest/woodland, temperate conifer forest, moist savannas, dry savannas, tall grassland, short grassland and xeric woodland/scrub, that are not in good agreement with the maps. Boreal deciduous forests/woodlands dominated by boreal summer-green trees occur naturally in northernmost China, in the southernmost Eurasian taiga zone in the area of Daxingan mountains. The model also predicted montane boreal biomes, although with a wider distribution than the mapped data, around the periphery of higher elevations on the Tibetan Plateau, the Tian and Altai mountains, and at some sites in the Changbai mountains.

Temperate conifer forest is simulated around the periphery of the temperate/boreal mixed forests in north-eastern China and central China where temperate conifers are the dominant trees. Warm–temperate conifers also dominate along the south-eastern slope of the Tibetan Plateau between warm–temperate evergreen broadleaved forest and alpine tundra.

Moist savannas are predicted in northern China and some areas of central China where there lies an ecotone between forest and grassland. They are also predicted to occur in the easternmost part of Taiwan Island and Hainan Island, and several areas of tropical south-western China. Dry savannas are predicted to be sparse in northern and north-western China mixed in three biomes: grassland, steppe and desert. Tall grassland is predicted on the edge of temperate/boreal forest, and in the areas of the Tian mountains and short grassland near tall grassland in northern China, around the Tian mountains and on the southern slope of the Altai mountains.

Xeric woodland/scrub is found in the river valley of south-western China, eastern Hainan Island and several coastal areas of southern China; however, the model only predicts a few grid cells in south-western China for this biome.

Ice/polar desert is shown for scattered grid cells in the Tibet and Tian mountains, more than in reality.

Response of vegetation distribution to climate change and elevated CO_2

If CO_2 emissions are maintained at near 1994 levels, then there would be a nearly constant rate of increase in atmospheric concentrations for at least two centuries, reaching about 500 p.p.m.v. (approaching twice the pre-industrial concentration of 280 p.p.m.v.) by the end of the 21st century (IPCC, 1996). Climate is expected, therefore, to continue to change into the future. According to the Hadley Climate Centre GCM output (Mitchell *et al.*, 1995; John *et al.*, 1997), annual mean temperature anomalies are expected to increase by between 2.2 and 4.4 °C by the end of the 21st century in China. The largest increases (3.4–4.4 °C) are expected to occur in cold–temperate areas (north-eastern and north-western China) and Hainan Island. Increases between 2.8 and 3.4 °C are likely in temperate regions (northern China, subtropics, southern and south-western China) and around the periphery of Tibet. The least change (2.2–2.8 °C) may occur in eastern China and central and south-eastern Tibet. The greatest increases are likely to be in the winter.

The pattern of precipitation in China is likely to change and these changes may well be different between regions. The annual precipitation anomaly ranges between a 506-mm decrease and a 290-mm increase. Annual precipitation in most areas of China is predicted to increase and the largest increment (> 150 mm) may occur in the eastern subtropical area and westernmost part of Tibet. In central China, however, there may be lower annual precipitation (0–100 mm less). The largest decrease in precipitation (100–500 mm) is predicted for south-western Tibet.

Comparisons using the ΔV statistic of simulated vegetation using the Hadley GCM anomalies, with CO_2 held at 340 p.p.m.v. (Fig. 2a) and CO_2 increased to 500 p.p.m.v. (Fig. 2b), along with the baseline biome simulation (Fig. 1b) were carried out. The values were 0.18 and 0.24, respectively, for comparisons between baseline simulations and changed-climate alone, and baseline and changed-climate simulations with increased CO_2 (Table 5, columns C and D).

Climate change alone produces a large reduction in the desert, alpine tundra and ice/polar desert (Table 6), and a general pole-ward shift of the boreal, temperate deciduous, warm–temperate evergreen and tropical forest belts (Table 6, Fig. 2a), with a decrease in boreal deciduous forest and the appearance of tropical deciduous forest. Boreal/temperate evergreen conifer forest expands in Tibet but mostly disappears in north-eastern China. Both of these effects are caused by direct effects of the temperature increase and precipitation changes under the changed climate. Grasslands, shrubland, steppe and savannas increase in area (Table 6), because increased temperature and water stress favour C_4 grasses over C_3 woody plants (Haxeltine, 1996).

Including the physiological effects of CO_2 leads to a marked decrease in the area occupied by moist savannas and desert (Table 6). This is due to C_3 plants becoming more competitive relative to C_4 grasses, and to a general reduction

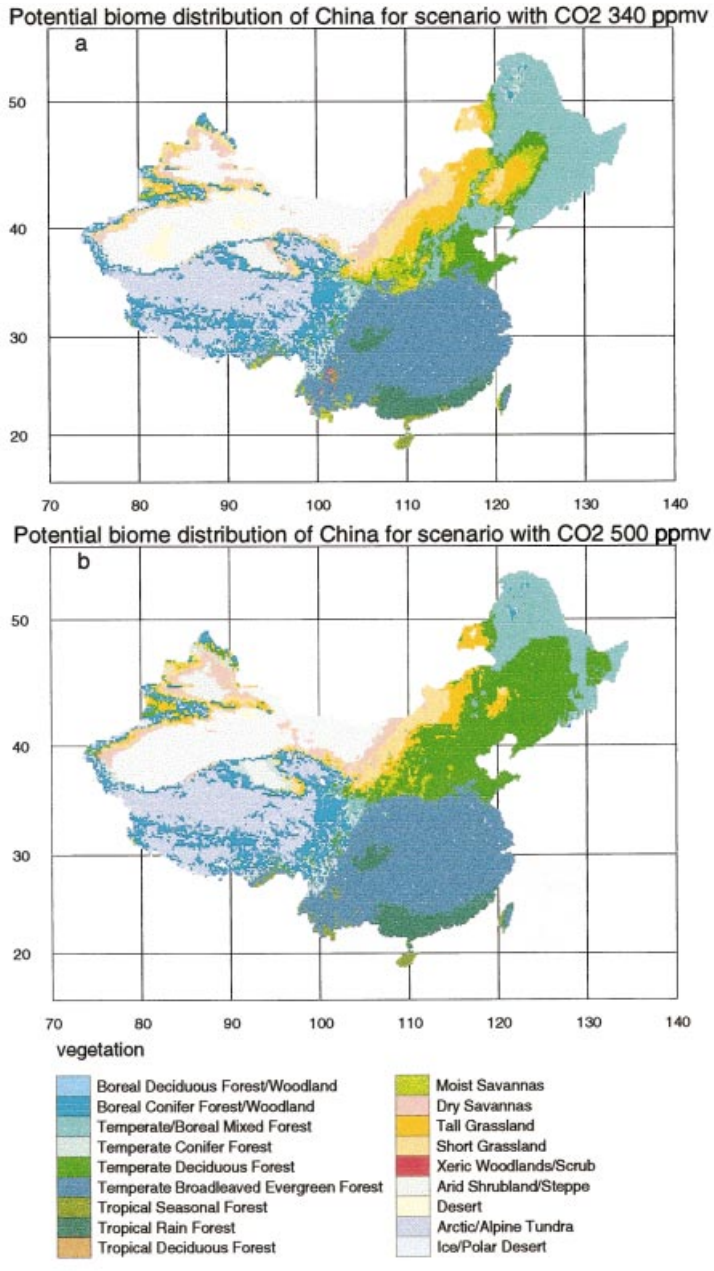

Fig. 2 Responses of mapped vegetation distribution to climate change and elevated CO_2. (a) Potential biome distribution of China as predicted by BIOME3 (Haxeltine & Prentice, 1996) without CO_2 effect; and (b) potential biome distribution of China as predicted by BIOME3 (Haxeltine & Prentice, 1996) with the direct effects of CO_2.

Table 6 Area covered by each biome for model simulations under: (A) present climate (B) enhanced CO_2 climate and (C) climatic scenario with inclusion of the direct effects of CO_2 on plant physiology

Biomes	Areas (10^3 km^2)		
	A	B	C
Boreal deciduous forest/woodland	1.39	0	1.11
Boreal evergreen forest/woodland	855.28	929.17	923.89
Temperate/boreal mixed forest	850.56	1154.17	628.33
Temperate conifer forest	282.78	184.72	222.78
Temperate deciduous forest	478.89	405.00	1512.22
Temperate broadleaved evergreen forest	1981.39	1991.11	2058.89
Tropical seasonal forest	45.83	66.94	76.11
Tropical rain forest	207.78	347.22	373.33
Tropical deciduous forest	0	8.33	0.56
Moist savannas	258.89	358.61	71.11
Dry savannas	191.94	266.39	272.78
Tall grassland	269.44	446.94	367.78
Short grassland	471.11	491.67	372.78
Xeric woodland/scrub	6.94	9.72	2.50
Arid shrubland/steppe	836.67	1341.11	1224.44
Desert	703.89	125.28	17.78
Arctic/alpine tundra	1747.50	1263.89	1263.89
Ice/polar desert	224.44	24.44	24.44

in stomatal conductance, which favours the dominance of woody plants by reducing water stress (Haxeltine, 1996). Eastern forest belts do not shift significantly to the north, apart from temperate deciduous broadleaved forest, which extends much further north and occupies nearly 50% of present-day temperate mixed forest areas (Fig. 2b). This is probably caused by high CO_2 concentration inducing more obvious reduction in stomatal conductance of broadleaved summergreens than that of coniferous evergreens and broadleaved evergreens.

NPP simulation and responses to changed climate and CO_2 enrichment

In addition to simulation of biome distributions, BIOME3 also predicts NPP of each grid cell. A comparison was made between predicted NPP and 690 site-based forest NPP field measurements (Ni *et al.*, unpublished data). There are many problems associated with such comparisons, including the quality of the data and the fact that the model is simulating the average NPP over a 10′ grid square while NPP measurements are made at particular sites (Haxeltine & Prentice, 1996). Despite these problems the resulting comparison shows an agreement between the predicted NPP and measurements (Fig. 3a: $y = 0.85x + 254.38$, $n = 690$, $r^2 = 0.31$).

Biome-averaged NPP comparison is more valuable than site-based NPP comparison. Higher correlation occurs in the biome-averaged comparison between field measured NPP and modelled NPP by BIOME3 (Fig. 3b: $y = 2.42x - 248.62$, $n = 16$, $r^2 = 0.82$). Modelled NPP of forest biomes, such as boreal evergreen forest/woodland, temperate/boreal mixed forest, temperate conifer forest, temperate deciduous forest, temperate broadleaved evergreen forest, tropical seasonal forest, and tropical rain forest, is larger than measured NPP in terms of biome averages (Fig. 3c) because BIOME3 simulated the average NPP of all vegetation types over a grid square. Modelled NPP of potential grassland, desert and tundra biomes predicted by BIOME3, such as moist savannas, dry savannas, tall grassland, short grassland, xeric woodland/scrub, arid shrubland/steppe, desert, and arctic/alpine tundra, where some forest types actually scatter, is less

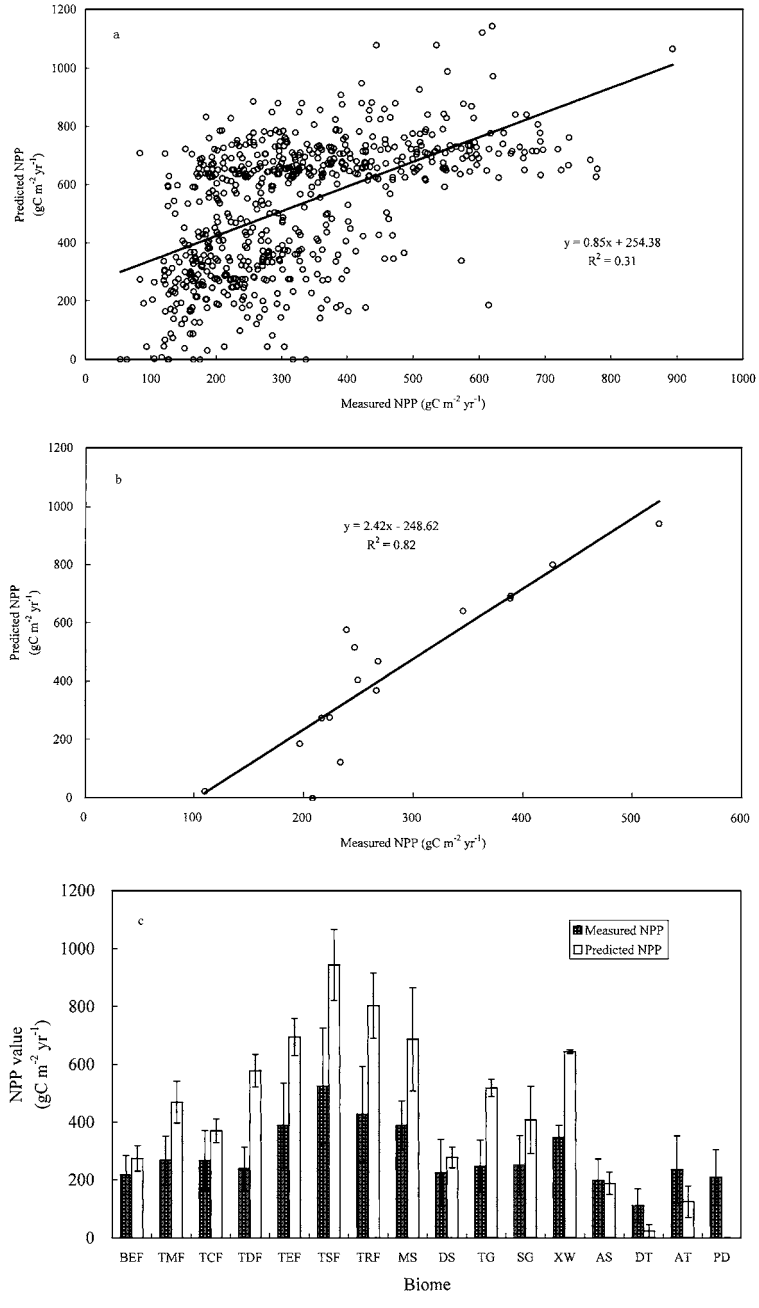

Fig. 3 Correlation between (a) site-based; (b) biome-averaged; and (c) relationships between NPP measurements and predictions in gC m^{-2} yr^{-1} by BIOME3 (Haxeltine & Prentice, 1996). The biomes are: BEF, boreal evergreen forest/woodland; TMF, temperate/boreal mixed forest; TCF, temperate conifer forest; TDF, temperate deciduous forest; TEF, temperate broadleaved evergreen forest; TSF, tropical seasonal forest; TRF, tropical rain forest; MS, moist savannas; DS, dry savannas; TG, tall grassland; SG, short grassland; XW, xeric woodland/scrub; AS, arid shrubland/steppe; DT, desert; AT, arctic/alpine tundra; and PD, ice/polar desert.

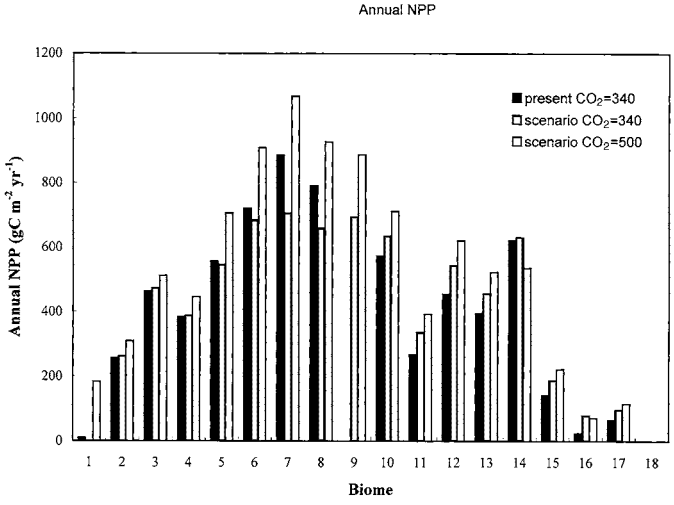

Fig. 4 Impacts of climate change and CO_2 concentration on NPP (gC m^{-2} yr^{-1}) for each biome. 1, Boreal deciduous forest/woodland; 2, boreal evergreen forest/woodland; 3, temperate/boreal mixed forest; 4, temperate conifer forest; 5, temperate deciduous forest; 6, temperate broadleaved evergreen forest; 7, tropical seasonal forest; 8, tropical rain forest; 9, tropical deciduous forest; 10, moist savannas; 11, dry savannas; 12, tall grassland; 13, short grassland; 14, xeric woodland/scrub; 15, arid shrubland/steppe; 16, desert; 17, arctic/alpine tundra; 18, ice/polar desert.

than measured NPP (Fig. 3c). The predicted ice/polar desert biome with positively measured forest NPP has zero modelled NPP on the Tibetan Plateau (Fig. 3a,c). These are sites at very high elevation with very low temperatures and BIOME3 seems to underestimate photosynthesis by arctic and alpine plants at low temperatures.

The impact of climate change and CO_2 is not only on the biogeography, but also on the biogeochemistry as represented by NPP. At current climate at 340 p.p.m.v. CO_2 concentration, the BIOME3 model estimates the total annual net primary production of the biomes to be between 0 and 1270.7 gC m^{-2} yr^{-1}. The highest productivity (800–1200 gC m^{-2} yr^{-1}) is found in tropical rain forest. Temperate forests have an intermediate NPP (500–800 gC m^{-2} yr^{-1}), while temperate savannas, grasslands and steppes have lower NPP values (200–500 gC m^{-2} yr^{-1}). The lowest NPP (< 200 gC m^{-2} yr^{-1}) is found in cold or arid regions, especially in the Tibetan Plateau, where temperature and/or precipitation are limiting.

For each biome, the predicted mean annual NPP varies between values for the current climate with CO_2 at 340 p.p.m.v., and a future scenario with CO_2 at 340 and at 500 p.p.m.v. (Fig. 4). The NPP values for most of the biomes in the scenario with CO_2 set at 340 p.p.m.v. are greater than those at the current climate with CO_2 at 340 p.p.m.v., except for the temperate deciduous forest, temperate evergreen broadleaved forest, tropical rain and seasonal forest biomes (Fig. 4). The NPP values for all biomes produced in the 500 ppmv CO_2 scenario (direct effects on physiology) are greater than those produced under the current climate, except for the xeric woodland/scrub biome (Fig. 4).

Using the medium carbon estimates based on biomass carbon densities from Prentice *et al.* (1993) and Olson *et al.* (1983), and soil carbon densities from Prentice *et al.* (1993) and Zinke *et al.* (1984), figures for the carbon storage of potential vegetation of 53.96×10^{12} gC in biomass and 117.84×10^{12} gC in soils were calculated. These figures are similar to the estimates, 57.73×10^{12} gC in biomass and 118.54×10^{12} gC in soils, for the predicted biomes by BIOME3 model. Applying the same carbon densities to biomes in future, total carbon in vegetation and soils will increase to 63.36 and 118.01×10^{12} gC

for the climate scenario without the CO_2 direct physiological effect, and to 69.43 and 122.76×10^{12} gC for the climate scenario with the CO_2 direct physiological effect, respectively.

DISCUSSION

The predictions from BIOME3 for Chinese biome distributions using new regional climate and soils data as well as a finer spatial resolution, gives a much improved agreement with natural vegetation distributions (cf. Haxeltine & Prentice, 1996). Some predictions, however, are still only in fair or poor agreement with natural vegetation. The reasons for these disagreements are as follows.

1 There remain problems of definitions of some biome types, e.g. the moist savannas, dry savannas, tall grassland and short grassland, as well as some discrepancies regarding the boundary of some biomes, such as between tropical rain forest and tropical seasonal forest. There also remain problems of the reclassification of the potential vegetation map based on bioclimatic criteria and BIOME3 output because some subjective judgement went into the reclassification.

2 The prediction of biome distributions is for potential vegetation, whereas the natural vegetation includes agricultural vegetation. If we compared the modelled biomes with potential vegetation divisions (Editorial Committee for Vegetation of China, 1980), some predicted biomes such as the moist savannas, dry savannas, tall grassland, and xeric woodland/scrub have much better agreement to potential vegetation division than actual vegetation distribution (Table 5, column B).

3 It may be necessary to increase the numbers of PFTs for Chinese simulations to distinguish some biomes, especially savannas and grasslands.

A doubled CO_2 climate, with and without the direct effects of CO_2, shifts biomes north and west. The largest changes occur in boreal evergreen forest/woodland, temperate conifer forest, xeric woodland/scrub, and alpine tundra and ice/polar desert. This occurs between their distribution under present climates and their distributions in doubled CO_2 climates without the direct effects of CO_2. However, boreal evergreen forest/woodland, moist savannas, dry savannas, tall grassland, xeric woodland/scrub, alpine tundra and ice/polar desert distributions change most between present climate and a doubled CO_2 climate with direct physiological effects. In general, climate change and the direct physiological effects of CO_2, as might be expected, produced more changes in distribution patterns than in the simulation only with a changing climate.

Vegetation and soil carbon values estimated by the carbon density method at present and in the next 100 years are based on the assumption of fixed carbon densities. However, the assumption relies on equilibrium, i.e. it is assumed that soil carbon has reached a constant value so that litterfall is exactly balanced by heterotrophic respiration. In reality this would take many hundreds of years. The classical values for vegetation carbon storage in the literature (Prentice *et al.*, 1993) are large. Also, the use of pre-assigned carbon densities would be ignoring the potential effects of changing CO_2 concentrations. Therefore, although we calculated potential carbon storage by the carbon density method for vegetation and soils, it would be more relevant to look at NPP, which is not subject to any long time lags.

It should be mentioned that the study used only one climate scenario, the Hadley Centre GCM, UK (Mitchell *et al.*, 1995; John *et al.*, 1997) for testing the potential sensitivity of Chinese ecosystems to changing climate and CO_2 concentrations. However, there are a number of different scenarios available and it is likely that they may give different results not only in the range and direction of biome shifts, and area of biome changes, but also in the values and ranges of NPP and carbon increase or decrease.

Climate changes are predicted to take place on a time-scale of a century or less, but the actual vegetation found under this new climate may be expected to be very different from potential natural vegetation as modelled, due to time lags associated with successional and migrational processes (Pitelka *et al.*, 1997), which are not modelled explicitly here.

As our activities continue to alter the planetary environment, it is essential that we improve our understanding of the terrestrial biosphere, not only in terms of the possible impacts of climate, but also in terms of the interactive role that biospheric processes play in the functioning of the Earth system as a whole (Foley *et al.*, 1996). Dynamic global vegetation models

(DGVMs), e.g. IBIS (Foley *et al.*, 1996), the Sheffield DGVM (Beerling *et al.*, 1997; Woodward & Beerling, 1997) and the LPJ DGVM (Sitch *et al*. in preparation) are being applied to regions such as China (Liu *et al*. in preparation). It remains to be seen what advantages they have over equilibrium models in our understanding of the processes occurring at the landscape and regional scale.

ACKNOWLEDGMENTS

The research presented in this paper was undertaken while Jian Ni was a guest scholar at the Department of Ecology, Plant Ecology, Lund University, Sweden, in the 1997/1998 academic year, with funding from the Swedish Institute (SI). We thank the Laboratory of Quantitative Vegetation Ecology (LQVE), Institute of Botany, the Chinese Academy of Sciences for providing Chinese climate, soils and vegetation data. Thanks to D.A. Yang and Z.Y. Yang in LQVE for technical assistance, Sharon Cowling, Ben Smith, Jed Kaplan, Alex Haxeltine, Kurt Olsson, Inger Josson, Tommy Olsson and Bo Wallen in the Department of Ecology, Plant Ecology, Lund University of Sweden for much help. Thanks also to Jon Foley and an anonymous reviewer for commenting on the manuscript. The research was jointly funded by the National Natural Science Foundation of China (NSFC no. 39700018, 39970154 & 49731020), and the Laboratory of Quantitative Vegetation Ecology, Institute of Botany, Chinese Academy of Sciences (LQVE no. LP9705).

REFERENCES

Beerling, D.J., Woodward, F.I., Lomas, M. & Jenkins, A.J. (1997) Testing the responses of a dynamic global vegetation model to environmental change: a comparison of observations and predictions. *Global Ecology and Biogeography Letters*, **6**, 439–450.

Chinese Central Meteorological Office (1984) *Climatological Data of China*. China Meteorology Press, Beijing.

Claussen, M. & Esch, M. (1994) Biomes computed from simulated climatologies. *Climate Dynamics*, **9**, 235–243.

Editorial Committee for Vegetation of China (1980) *Vegetation of China*. Science Press, Beijing.

Foley, J.A., Prentice, I.C., Ramankutty, N., Levis, S., Pollard, D., Sitch, S. & Haxeltine, A. (1996) An integrated biosphere model of land surface processes, terrestrial carbon balance, and vegetation dynamics. *Global Biogeochemical Cycles*, **10**, 603–628.

Haxeltine, A. (1996) Response of global vegetation distribution and net primary production to climate change. Modelling the vegetation of the world. PhD Thesis, 124 pp. Lund University Press, Lund.

Haxeltine, A., Prentice, I.C. & Cresswell, I.D. (1996) A coupled carbon and water flux model to predict vegetation structure. *Journal of Vegetation Science*, **7**, 651–666.

Haxeltine, A. & Prentice, I.C. (1996) BIOME3: an equilibrium terrestrial biosphere model based on ecophysiological constraints, resource availability and competition among plant functional types. *Global Biogeochemical Cycles*, **10**, 693–709.

Hou, X.Y., Sun, S.Z., Zhang, J.W., He, M.G., Wang, Y.F., Kong, D.Z. & Wang, S.Q. (1982) *Vegetation Map of the People's Republic of China*. China Map Publisher, Beijing.

Hulme, M., Wigley, T., Jiang, T., Zhao, Z.C., Wang, F.T., Ding, Y.H., Leemans, R. & Markham, A. (1992) *Climate Change Due to the Greenhouse Effect and its Implications for China*. WWF Report, Gland.

Hutchinson, M.F. (1989) A new objective method for spatial interpolation of meteorological variables from irregular networks applied to the estimation of monthly mean solar radiation, temperature, precipitation and windrun. *Need for Climatic and Hydrologic Data in Agriculture in Southeast Asia*. CSIRO, Canberra.

Intergovernmental Panel on Climate Change (IPCC) (1996) *Climate Change 1995: the Science of Climate Change*. Cambridge University Press, Cambridge.

Johns, T.C., Carnell, R.E., Crossley, J.F., Gregory, J.M., Mitchell, J.F.B., Senior, C.A., Tett, S.F.B. & Wood, R.A. (1997) The second Hadley Centre coupled ocean–atmosphere GCM: model description, spinup and validation. *Climate Dynamics*, **13**, 103–134.

Melillo, J.M., McGuire, A.D., Kicklighter, D.W., Moore, B. III, Vorosmarty, C.J. & Schloss, A.L. (1993) Global climate change and terrestrial net primary production. *Nature*, **363**, 234–240.

Melillo, J.M. (1995) Terrestrial biosphere–atmosphere system: a challenge for IGBP and WCRP. *Global Analysis, Interpretation and Modelling (GAIM): towards an integration of global systems science* (ed. by B. Morre III & D. Sahagian). Cambridge University Press, Cambridge.

Melillo, J.M., Prentice, I.C., Schulze, E.-D., Farquhar, G.D. & Sala, O.E. (1996) Terrestrial ecosystems: biotic feedbacks to climate. *Climate Change: the IPCC 1995 Assessment* (ed. by J.T. Houghton, L.G. Meira Filho, B.A. Callander, N. Harris, A. Kattenberg & K. Maskell), pp. 449–481. Cambridge University Press, Cambridge.

Mitchell, J.F.B., Johns, T.C., Gregory, J.M. & Tett, S.F.B. (1995) Climate response to increasing levels of greenhouse gases and sulphate aerosols. *Nature*, **376**, 501–504.

Monserud, R.A. & Leemans, R. (1992) Comparing global vegetation maps with the Kappa statistic. *Ecological Modelling*, **62**, 275–293.

Olson, J.S., Watts, J.A. & Allison, L.J. (1983) *Carbon in live vegetation of major world ecosystems*. ORNL-5862. Oak Ridge National Laboratory, Oak Ridge.

Pitelka, L.F. & the Plant Migration Workshop Group. (1997) Plant migration and climate change. *American Scientist*, **85**, 464–473.

Prentice, I.C., Cramer, W., Harrison, S.P., Leemans, R., Monserud, R.A. & Solomon, A.M. (1992) A global biome model based on plant physiology and dominance, soil properties and climate. *Journal of Biogeography*, **19**, 117–134.

Prentice, I.C., Sykes, M.T., Lautenschlager, M., Harrison, S.P., Dennissenko, O. & Bartlein, P.J. (1993) Modelling global vegetation patterns and terrestrial carbon storage at the last glacial maximum. *Global Ecology and Biogeography Letters*, **3**, 67–76.

Prentice, I.C. & Sykes, M.T. (1995) Vegetation geography and global carbon storage changes. *Biotic Feedbacks in the Global Climatic System: will the warming speed the warming?* (ed. by G.M. Woodwell & F.T. Mackenzie), pp. 235–236, Oxford University Press, New York.

Smith, T.M., Shugart, H.H., Bonan, G.B. & Smith, J.B. (1992) Modelling the potential response of vegetation to global climate change. *Advances in Ecological Research*, **22**, 93–116.

Sykes, M.T., Prentice, I.C. & Laarif, F. (1999) Quantifying the impact of global climate change on potential natural vegetation. *Climatic Change*, **41**, 37–52.

VEMAP Members (1995) Vegetation/Ecosystem Mapping and Analysis Project (VEMAP): a comparison of biogeography and biogeochemistry models in the context of global change. *Global Biogeochemical Cycles*, **9**, 407–437.

Woodward, F.I. & Beerling, D.J. (1997) The dynamics of vegetation change: health warmings for equilibrium 'Dodo' models. *Global Ecology and Biogeography Letters*, **6**, 413–418.

Xiong, Y. & Li, Q.K. (1987) *Soil of China*, 2nd edn. Science Press, Beijing.

Zhang, X.S. & Yang, D.A. (1993) A study on climate–vegetation interaction in China: the ecological model for global change. *Coenoses*, **8**, 105–119.

Zhang, X.S. & Yang, D.A. (1990) The radiative dryness index and potential productivity of vegetation in China. *Journal of Environmental Sciences (China)*, **2**, 95–109.

Zinke, P.J., Stangenberger, A.G., Post, W.M., Emanuel, W.R. & Olson, J.S. (1984) *Worldwide organic soil carbon and nitrogen data*. ORNL/TM-8857. Oak Ridge National Laboratory, Oak Ridge.